

IL NUOVO CIMENTO  
DOI 10.1393/ncc/i2011-10992-8

VOL. 34 C, N. 5

Settembre-Ottobre 2011

COMMUNICATIONS: SIF Congress 2010

## Complex depletion forces

S. BUZZACCARO(\*)

*Dipartimento di Chimica, Materiali e Ingegneria Chimica (CMIC), Politecnico di Milano  
via Ponzio 34/3, 20133 Milano, Italy*

(ricevuto il 31 Dicembre 2010; approvato il 3 Febbraio 2011; pubblicato online il 5 Ottobre 2011)

**Summary.** — Most experimental studies of the effects of depletion forces in a colloidal suspensions have so far been performed on systems where the depletion agent can be regarded as ideal. Here, we review our recent results on systems where depletants present self-interactions. In the first case we focus on a system where strong electrostatic coupling is present in the suspension. At fixed colloid volume fraction, colloidal aggregation takes place when the surfactant concentration reaches a critical value which raises for increasing ionic strength. Screening repulsive electrostatic interactions inhibits the depletion mechanism and weakens the effective colloid-colloid attraction. In the second case, investigating the depletion effects brought in by surfactants that show a liquid-liquid phase separation with water, we shall conversely deal with a situation where long-range spatial correlations are of primary importance in setting the phase behavior of the colloidal fluid. Our experimental and theoretical results show that, in the proximity of the critical demixing point, depletion effects merge continuously into critical Casimir effects, displaying distinctive scaling properties.

PACS 82.70.Dd – Colloids.

PACS 82.70.Uv – Surfactants, micellar solutions, vesicles, lamellae, amphiphilic systems, (hydrophilic and hydrophobic interactions).

PACS 05.70.Ce – Thermodynamic functions and equations of state.

PACS 05.70.Jk – Critical point phenomena.

### 1. – Introduction

Colloidal particles dispersed in a medium encompass a large class of complex fluids. In these systems the addition of other smaller components as polymers, salt, surfactant molecules that can self-aggregate forming micelles, induces effective interactions between the bigger solid particles. This ability of easily tuning particles interaction has made colloidal dispersion one of the most useful experimental system in order to prove liquid

(\*) E-mail: stefano.buzzaccaro@mail.polimi.it

state theory. In this field the investigation of systems of colloidal particles interacting via very short-ranged (much smaller than particle radius) attractive forces has yielded valuable and often unforeseen insights into the contingency of the liquid state and into the origin of metastable gel or glassy phases [1-3]. In this regard, the Adhesive Hard Spheres (AHS) limit [4], corresponding to an attractive potential of vanishing range  $u(r)/k_B T = -\ln[\sigma\delta(r - \sigma)/12\tau]$ , where  $\sigma$  is the particle diameter and  $\tau$  is a “stickiness parameter”, has become the paragon model. Short-ranged interactions can be induced by the addition into the colloidal suspension of *small* non-adsorbing components (polymers, micelles, spheres...): when two big particles of radius  $R$  approach until the center-to-center distance is smaller than the typical size of the added component, this will be ejected from the overlap volume. The pressure unbalance generates a net attraction between the big particles. This kind of forces is commonly called “depletion interactions”. Recently [4] we investigated the full equation of state of a system of AHS, in which interactions are induced by the addition of a non-ionic surfactant (Triton X100), in order to inspect fine details of the phase diagram, and to provide quantitative information on the structure and elastic properties of gel phases. It is useful briefly recall some qualitative observation made in this latter study. Depending on the micellar volume fraction  $\Phi_s$ , the samples display two radically different kinds of behavior. While for  $\Phi_s < 0.105$  they remain transparent and sediment very slow, samples with higher surfactant concentration show a sudden increase of turbidity, witnessing strong fluctuations of concentration, followed by rapid settling, leading in a few hour to the formation of a dense sediment. The transition between these two different regimes is abrupt and reversible: An increase by less than  $\Delta\Phi_s = 0.007$  in micellar volume fraction leads a transparent sample to become turbid and sediment fast. The Noro-Frenkel generalized law of corresponding states [5], stating that all short-ranged spherically symmetric attractive potentials are characterized by the same thermodynamics properties if compared at the same reduced density and virial coefficient, was then used to map the experimental phase boundaries onto the phase diagram predicted for short-ranged depletion potential with the very small range set by the micelle/particle size ratio. The most noticeable feature of the results presented in [4] is that *all* rapidly settling samples are placed within, or very close to, the metastable liquid-liquid (L-L) separation gap in the theoretical phase diagram [6], suggesting to regard gelation as an arrested phase-separation process. *Fast sedimentation can be therefore regarded as a basic clue for locating the L-L phase separation boundary*, a crucial observation that will be a guiding line for the present paper. Triton micelles behave as an ideal gas and do not interact. In this case it was possible to derive an exact expression for the force, the celebrated Asakura-Oosawa [7] formula, which is rightly considered a paradigmatic description of the depletion interaction. However, in real systems the depletion agent, that is the fluid hosting the colloidal particles, is often far from being an ideal gas and in those cases the Asakura-Oosawa formula is a crude approximation. This opens up a totally new question, which we could summarize as follows: *What is the behavior of a colloidal suspensions in an effective solvent, made of a solution of much smaller colloids which have a generic self-interactions?* From the theoretical point of view, this amounts to investigating whether the classical McMillan-Mayer approach to the potential of the mean force can be extended to yield general ideas on the phase behavior of mesoscopic particles in such a structured solvent. Sticking to depletion interactions, the problem is far from being trivial. Consider for instance only repulsive self-interactions of the depletant. On the one hand, its osmotic pressure increases, so that depletion forces on the colloids become stronger. On the other, however, the depletant gets structured, and this has been shown to reduce depletion. According to

urban myth, at least for binary Hard Spheres, this second contribution eventually wins, so that depletion is weaker than in the ideal case. But the theoretical results have been grossly overlooked. A more careful analysis shows that there is a subtle effect of the depletant/particle size ratio: in fact, for very small size, the opposite is true. When the repulsive self-interactions are longer range, as for electrostatic forces, the osmotic effect becomes even more dominant [8]. In the next section indeed, we give ample evidence that depletion interactions using a charged depletant (SDS) becomes much stronger, to the extent that even a tiny amount of surfactant is sufficient to phase-separate the colloids. An even more interesting question concerns the effect of strong attractive forces between the depletant. Here the depletant osmotic pressure decreases, so that one should get weaker depletion. But structuring effects play a strongly conflicting role, increasing in this case depletion forces. As is well known, the surfactant micelles of a non-ionic surfactant, which at room temperature behave almost as an ideal gas, show an inverted consolution curve with water at high (but accessible)  $T$ . In the second part of the paper we demonstrate that if one then add colloids, the amount of surfactant needed to phase-separate the colloids strongly decreases by increasing  $T$  and approaching the surfactant-water consolution curve: this trend is strongly correlated with the growth of the correlation length of the micellar solution [9-11]. The idea that fluctuations between two macroscopic bodies can induce a force of attraction (or repulsion) between them originates from the work of Casimir [12] who recognized that two parallel metallic plates placed a distance  $L$  apart in vacuum experience a force of attraction due to the zero-point fluctuations of the electromagnetic field. Thirty years ago, Fisher and de Gennes [13] demonstrated using the scaling theory that, if the fluid confined between the dielectric plates exhibits long-ranged critical fluctuations, then an additional *critical Casimir force* must exist. Our experimental result and its theoretical interpretation strongly suggest that a deep relation exists between depletion forces and the critical Casimir effect. In fact, depletion merges continuously into critical Casimir effect, fully sharing its scaling properties and allowing to speak of “Critical Depletion” [9].

## 2. – Charged depletant

The aim of this section is highlighting and quantitatively accounting for additional depletion attraction that is actually brought in by repulsive Coulomb interactions between the components. A more detailed discussion can be found in [8].

### 2.1. *Materials and experimental methods*

*Colloidal system.* The colloids we have used in both the experiments described in the present paper are aqueous suspensions of Hyflon<sup>TM</sup> MFA, a copolymer of tetrafluoroethylene (TFE) and perfluoromethylvinylether (PF-MVE) produced by Solvay-Solexis (Bollate, Italy). While pure polytetrafluoroethylene (PFTE) is almost a fully crystalline polymer, usually forming by emulsion polymerization polydisperse rod-shaped particles, the addition of PF-MVE, bestowing a larger flexibility to the chains, yields spherical, monodisperse particles, which can be envisioned as a polycrystalline assembly embedded into an amorphous matrix [14]. For the particle we have used to investigate charged depletant effects, Dynamic Light Scattering (DLS) yields an average radius of 90 nm and a polydispersity of about 4%. The surface of MFA latex particles bears a negative charge, mostly due to the presence of trapped fluorinated surfactant used in the emulsion polymerization and, possibly, to added ionic stabilizers. In all what follows,

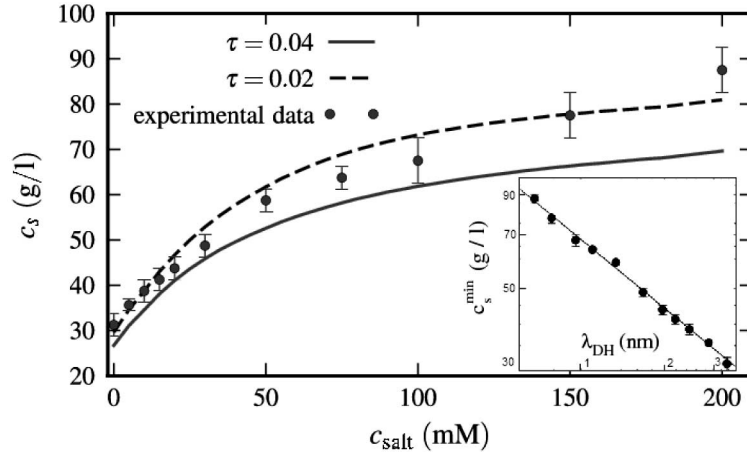


Fig. 1. – Phase transition curve of MFA with SDS depletant as a function of added salt (full dots). The curves correspond to theoretical predictions, obtained from the mapping onto the Baxter model, corresponding to two different values of the critical  $\tau$ . The data are plotted in the double-log inset as a function of  $\lambda_{DH}$ , with a power-law fit.

therefore, we shall assume the bare MFA particle charge is high enough to fully satisfy the requirements for charge renormalization.

*Depletion agent.* The experiments have been performed using as a depletion agent sodium dodecyl sulfate (SDS). The physical properties of aqueous solutions of SDS, a simple anionic surfactant with molecular weight  $M_{sds} = 288$  Da, have been extensively investigated in the past [15]. Beyond a critical micellar concentration (cmc) that depends on the ionic strength  $I$  (decreasing from 8.3 mM in pure water to 0.9 mM for  $I = 200$  mM), SDS forms globular micelles with a pretty constant hydrodynamic radius  $a \simeq 2.5$  nm. Their aggregation number  $N$ , and therefore structural charge  $Z$ , is around 80–110, varying by no more than  $\pm 10\%$  up to an ionic strength  $I \simeq 0.4$  M, beyond which the micellar morphology becomes elongated and  $N$  grows consistently.

**2.2. Phase separation line.** – Aiming to unravel phase separation effects in the presence of a charged depletant, we consider the dependence of the minimal micellar volume fraction  $c_s^{min}$  required to induce rapid phase separation as a function of the solution ionic strength, varied by the addition of NaCl. Samples were prepared at several different values of the salt concentration, at fixed particle volume fraction  $\Phi = 0.02$ . The value of  $c_s^{min}$  was fixed by visually checking for rapid sedimentation effects, which indicates those samples lying within the unstable region. Actually, the critical micellar concentration in the absence of added salt sets a lower limit of about 8 mM for the minimum ionic strength that can be reached in the experiments, limiting therefore the Debye-Hückel length to a value  $\lambda_{DH} < 3.5$  nm, which is comparable to the size of a SDS micelle, but *much smaller* than the colloid radius. We assume that the surfactant concentration in micellar form  $c_s$  (in g/l) is given by the difference between the amount of the surfactant actually added to the solvent and the (ionic strength dependent) critical micelle concentration (cmc). The experimental results, presented in fig. 1, show that all samples displayed a sharp value for  $c_s^{min}$ , even at the lowest accessible ionic strength, which however decreases by decreasing

the salt concentration, witnessing a consistent *increase* of depletion efficiency at low ionic strength. The inset show also that, at least within this ionic strength range,  $c_s^{min}$  displays an approximately power-law trend with the Debye screening length,  $c_s^{min} = a\lambda_{DH}^{-b}$ , with a phenomenological exponent which is around  $b \simeq 0.6$ .

In the following we attempt an interpretation of the experimental results in the framework of classical statistical mechanics and liquid state theory, starting from a microscopic description of the colloidal suspension.

**2.3. Theoretical analysis.** – We consider a homogeneous dispersion of colloids and micelles in an electrolyte at room temperature. Here and in the following the subscripts  $b$  and  $s$  will denote quantities related to the colloids (the *big* species) and the micelles (the *small* species), respectively, whereas the Greek indices  $\mu$  and  $\nu$  will be used to refer either species.

Both the colloids and the micelles are represented as charged hard spherical particles, neglecting dispersion forces, with diameter  $\sigma_\mu$ , radius  $a_\mu = \sigma_\mu/2$  and number density  $n_\mu$  carrying a net negative charge  $-Z_\mu e$ ,  $e$  being the elementary charge. Electrostatic interactions in colloidal dispersions are deeply affected by screening from mobile charges in the solution, which include: positive and negative ions resulting from the dissolution of a salt of bulk molar concentration  $c_{salt}$ ; the cmc contribution due to free SDS surfactant molecules; positive counterions released by the colloids and the micelles. In the following we will neglect the colloid counterions because their contribution is always negligible at the concentrations we investigated. The relevant parameter governing the amount of mobile charges is the ionic strength  $I = c_{salt} + cmc + \frac{Z_s^{eff} n_s}{2N_A}$ , where  $N_A$  is the Avogadro number and  $Z_s^{eff}$  is the number of *mobile* counterions released by each micelle.

A key quantity characterizing the screening cloud at a surface is the inverse Debye length  $\kappa = \sqrt{8\pi l_B N_A I}$ ,  $\beta$  is the inverse thermal energy and  $\epsilon$  is the relative permittivity of the solvent. In the parameter range of our experiments the Debye length is the smallest length-scale in our problem. In order to calculate an effective colloid-colloid interaction mediated by the micelles we have to define the micelle-micelle ( $v_{ss}(r)$ ), colloid-colloid ( $v_{bb}(r)$ ) and micelle-colloid ( $v_{bs}(r)$ ) direct interaction potentials:

- We will therefore model the micelles through a purely repulsive interaction  $v_{ss}(r)$  comprising hard sphere exclusion and Coulomb repulsion, represented in the Yukawa form:

$$(1) \quad \beta v^{DH}(r) = \frac{a}{2l_B} y_s^2 \frac{\exp[-\kappa(r - \sigma)]}{r/\sigma},$$

where the amplitude  $y_s$  provides the effective surface potential.

- The electrostatic energy of interaction of two colloidal particles, whose radii are much larger than the screening length, is usually modeled within Derjaguin approximation [16]:

$$(2) \quad \beta v_{bb}(r) = \frac{a_b}{2l_B} y_b^2 \log \left[ 1 + e^{-\kappa(r - \sigma_b)} \right],$$

in the physically accessible region  $r > \sigma_b$ , where  $y_b \sim 4$ .

– The colloid-micelle interaction is described by the Hogg-Healy-Fuerstenau form [17]:

$$(3) \quad \beta v_{bs}(h) = \frac{1}{4l_B} \frac{a_b a_s}{a_b + a_s + h} \left[ 4y_b y_s \operatorname{atanh}(e^{-\kappa h}) - (y_b^2 + y_s^2) \log(1 - e^{-2\kappa h}) \right].$$

Once defined  $v_{\mu\nu}(r)$ , a common way to obtain the effective potential is to calculate the free energy of the small particles at fixed configuration of the big ones. Here we employ an approach based on integral equations from the theory of simple liquids. It is known that in a homogeneous one-component fluid the zero density limit of the radial distribution function equals the Boltzmann factor of the two-body term in the interaction potential [18]. The same property holds in the mixture:

$$(4) \quad \lim_{n_b \rightarrow 0} g_{bb}(r; n_b, z_s) = \exp \left[ -\beta [v_{bb}(r) + w^{(2)}(r; z_2)] \right] \doteq \exp[-\beta V^{\text{eff}}(r; z_s)],$$

where  $g_{bb}$  is the radial distribution function of the large particles and we defined  $V^{\text{eff}}$  as the two-body term of the effective potential. Thus, the latter is known once the correlations between the particles in the mixture are calculated at the pair level.

To obtain the correlations, we consider the Ornstein-Zernike relations for the mixture [18] in the limit of vanishing density of the large particles:

$$(5a) \quad h_{ss}(r) = c_{ss}(r) + n_s^r [c_{ss} * h_{ss}](r),$$

$$(5b) \quad h_{bs}(r) = c_{bs}(r) + n_s^r [c_{bs} * h_{ss}](r),$$

$$(5c) \quad h_{bb}(r) = c_{bb}(r) + n_s^r [c_{bs} * h_{sb}](r);$$

here,  $h_{\mu\nu} = g_{\mu\nu} - 1$  and  $c_{\mu\nu}$  are the sets of total and direct correlation functions, the symbol  $*$  denotes the three-dimensional product of convolution and  $n_s^r$  is the so-called reservoir density of the small particles, defined as the density of particles in a system comprising the small species alone in osmotic equilibrium with the mixture at a given composition. We supplement the Ornstein-Zernike equations (5) with the hypernetted-chain (HNC) closure [18]:

$$(6) \quad \log g_{\mu\nu}(r) = -\beta v_{\mu\nu}(r) + h_{\mu\nu}(r) - c_{\mu\nu}(r).$$

Once the effective pair potential  $V^{\text{eff}}$  is calculated, the thermodynamic properties of the effective one-component fluid comprising the big particles alone can be obtained by several methods. When dealing with short-ranged interactions in colloidal systems, the Noro-Frenkel extended law of corresponding states is usually invoked: the compressibility factor is a universal function of the reduced temperature, density and of the reduced second virial coefficient  $B_2^*$ , but is independent of the specific shape of the potential [5]. Thus, the properties of the system of interest can be mapped onto those of an adhesive-hard-sphere fluid with a stickiness parameter  $\tau$  corresponding to the given  $B_2^*$  [4]. Values of  $\tau$  close to zero signal strong adhesion between the big particles, whereas large values point out a behavior akin to hard spheres.  $\tau$  is defined in terms of the second virial coefficient of the colloids as  $\tau = 1/(4 - B_2^*)$ . The sticky sphere model has been extensively investigated in the past [6] and its phase diagram is by now well known leading, via the Noro-Frenkel scaling, to a simple way to investigate the thermodynamic properties of this class of systems. If the experimentally observed aggregation of the colloidal

particles is interpreted as a thermodynamic instability driven by the divergence of the isothermal compressibility, then the experimental transition points in the  $(c_{\text{salt}}, c_s)$ -plane shown in fig. 1 should correspond to the spinodal boundary at a fixed colloid volume fraction  $\Phi_b = 0.02$ . From the Monte Carlo simulations in ref. [6] we can approximately locate the transition point at a stickiness parameter  $\tau$  in the range 0.04–0.08. The dependence of  $\tau$  on the physically accessible quantities  $(c_{\text{salt}}, c_s)$  has been evaluated from our effective colloid potential at different ionic strengths and surfactant concentrations. The results of the predicted transition line, evaluated for  $\tau = 0.02$  and  $\tau = 0.04$ , are shown in fig. 1 together with the experimental data. Due to the uncertainties in the parameters and the simplifications of the adopted model only a semi-quantitative agreement can be obtained. However, the experimentally observed trend is clearly present also in our model which in fact displays an enhanced tendency towards colloid aggregation when the electrostatic repulsion is poorly screened (at low ionic strength).

### 3. – Critical depletion

In this section, by investigating depletion interactions in colloidal suspensions characterized by a depletant with a miscibility gap, we show that Depletion Force and colloid phase separation close to a critical demixing point of the solvent (Critical Casimir Force) are two effects intimately connected. A more detailed analysis can be found in [9, 10].

#### 3.1. *Materials and experimental methods*

*Depletion agent.* As depletion agent, we have used  $\text{C}_{12}\text{E}_8$  (octaethylene glycol monododecyl ether), a nonionic surfactant, with molecular weight  $M_w = 538.75$  g/mol and a density very close to  $1$  g/cm<sup>3</sup>, belonging to the class of ethoxylate alcohols  $\text{C}_m\text{E}_n$ , where  $m$  is the number of carbon atoms in the hydrophobic chain, and  $n$  is the number of ethoxylate groups constituting the hydrophilic head group. Beyond its critical micellar concentration  $\text{cmc} = 0.038$  g/l ( $\simeq 71$   $\mu\text{M}$ , [19]),  $\text{C}_{12}\text{E}_8$  forms at room temperature globular micelles with a radius  $a = 3.4$  nm and an aggregation number  $N \simeq 95$ –100 as determined by both light [19] and neutron [20] scattering. Experiments are performed in the presence of 250 mM of NaCl in order to screen electrostatic interactions. As many nonionic surfactants,  $\text{C}_{12}\text{E}_8$  shows an inverted consolution gap with water, with a critical concentration  $c_c \simeq 1.8\%$  and a lower critical solution temperature that is  $T_c \simeq 64.5^\circ\text{C}$ . Thus, compared to simple critical mixtures, the critical concentration of  $\text{C}_{12}\text{E}_8$  is very low and the critical (osmotic) pressure is vanishingly small. Approaching the critical point amounts to inducing effective attractive interactions between the  $\text{C}_{12}\text{E}_8$  micelles, which can be detected and quantified by light scattering. Hence,  $\text{C}_{12}\text{E}_8$  can no longer be regarded as an ideal depletant, and the simple Asakura-Oosawa model is not expected to yield meaningful results.

*3.2. Phase separation line.* – We may then inquire, as in the previous section, whether and how the minimum amount of surfactant  $c_s$  needed to induce particle phase separation depends on  $T$ . Figure 2 shows that  $c_s$  noticeably decreases by increasing  $T$ , approaching the value  $c_s \simeq c_c$  for  $T \rightarrow T_c$ . The transition points are interpreted as signature of the crossing of the G-L coexistence line in the colloid phase diagram. According to the Noro-Frenkel principle [5] of corresponding states, these points are then associated to the same value  $B_2^* \simeq -6$  for the dimensionless second virial coefficient of the particle effective interaction. Close to  $T_c$  the interactions between  $\text{C}_{12}\text{E}_8$  micelles become

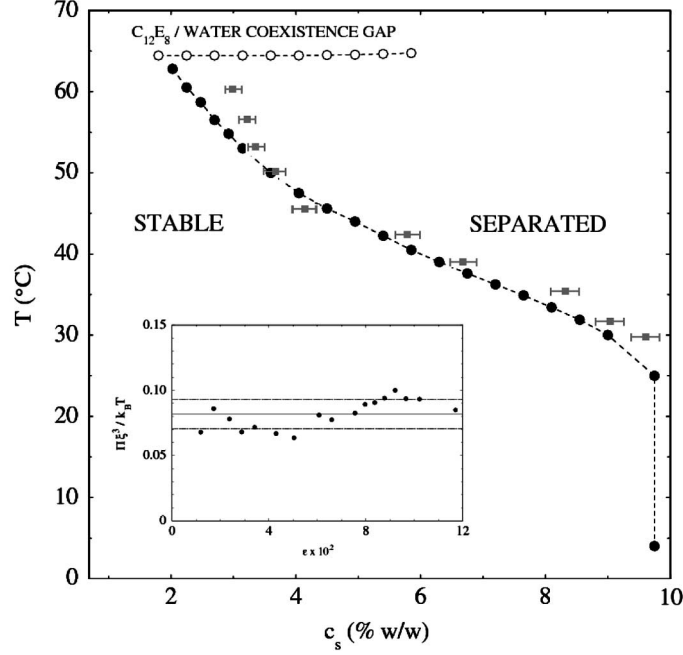


Fig. 2. – Minimum amount of surfactant  $c_s$  needed to induce phase separation for aqueous MFA suspensions (full dots). The consolusion curve of the surfactant solution is shown by open dots. Full squares represent maxima of the isothermal susceptibility. The inset shows the quantity  $\Pi\xi^3$  plotted *vs.* the reduced temperature, together with its average value (full line) and 1 standard deviation bounds (dashed lines).

strongly attractive, thus their osmotic pressure  $\Pi(c_s, T_s)$  is much smaller than for an ideal solution at the same concentration. Since in the simple Asakura-Oosawa picture the strength of the depletion attractive potential is proportional to  $\Pi(c_s, T_s)$ , this sensible decrease in  $c_s$  must be attributed to noticeable nonideality effect, and, in particular, to the growth of critical fluctuations. The osmotic pressure  $\Pi(c_s, T_s)$  of the (particle-free) surfactant solution at those values  $(c_s, T_s)$  corresponding to the state points in fig. 2 can be obtained by integrating the osmotic isothermal compressibility, measured up to  $c_s$  by light scattering. Data show that, sufficiently close to  $T_c$ , the difference  $c_s - c_c$  approximately behaves as a power law  $c_s - c_c \propto \Pi(c_s, T_s)^{2/3}$  [9, 10], having neglected the extremely small contribution coming from the osmotic pressure at the critical point. Moreover, within the critical region all physical properties should solely depend on the diverging correlation length  $\xi$  which can be readily evaluated from the diffusion constant  $D$  measured by dynamic light scattering as  $\xi = k_B T / 6\pi\eta D$ , where  $\eta$  is the viscosity of the solution. Exactly at state point  $(c_s, T_s)$  data shows that  $c_s - c_c$  also scales as a power law  $c_s - c_c \propto \xi(c_s, T_s)^{-1.8}$  [9, 10]. The two empirical trends we found imply that, along the transition line, the product  $\Pi\xi^3$  should depend very weakly on temperature. The inset in fig. 2 shows that this is actually the case in the whole temperature range investigated.

**3.3. Theoretical analysis.** – To rationalize these evidences, a basic picture of depletion effects in correlated fluids is therefore required. Following the McMillan-Mayer approach,



we will model the depletant as a simple fluid with some solvent mediated interaction identifying pressure and packing fraction of this fluid with the osmotic pressure  $\Pi$  and the concentration  $c_s$  of the original surfactant solution. We will employ Density Functional Theory (DFT) [18] to obtain a formally exact expression for the effective interaction. If we denote by  $A[n(\mathbf{r})]$  the Helmholtz free energy of the fluid at fixed density profile  $n(\mathbf{r})$ , we define the grand free energy functional  $\Omega[n(\mathbf{r})]$  as

$$(7) \quad \Omega[n(\mathbf{r})] = A[n(\mathbf{r})] + \int d\mathbf{r} \{ \Phi(\mathbf{r}) - \mu \} n(\mathbf{r})$$

by including the bulk fluid chemical potential  $\mu$  and the (external) wall-fluid interaction  $\Phi(\mathbf{r}) = w(z - \frac{h}{2}) + w(z + \frac{h}{2})$ . According to the Hohenberg-Kohn theorem [18] the equilibrium profile  $n(\mathbf{r})$  is determined by the extremum condition  $\delta\Omega[n(\mathbf{r})]/\delta n(\mathbf{r}) = 0$ .

To provide a quantitative evaluation of the effective depletion force  $F(h)$  we must now introduce some approximation in this formally exact theoretical framework. *In primis* we adopt the quasi-planar Derjaguin approximation, which is valid provided that the distance  $h$  between the two colloid surfaces  $S$  is much smaller than the colloid radius  $R$ . With this approximation the problem becomes monodimensional. A simple density functional able to capture both the AO low density, uncorrelated limit and the scaling form of the critical Casimir effect is provided by the local potential approximation. To discuss the long-range tails of the effective interaction, we adopt an expression for the density functional  $A[n(z)]$  appropriate for describing *long-wavelength density fluctuations* [21,22]:

$$(8) \quad A[n(z)] = \int dz \left[ \frac{b}{2} \left| \frac{dn(z)}{dz} \right|^2 + f(n(z)) \right].$$

This form corresponds to a local density approximation plus gradient corrections, where the parameter  $b$  measures the stiffness of the fluid with respect to density fluctuations. In a critical fluid, long-range fluctuations yield a scaling form for the singular part of the free-energy density:  $f(n) \propto \epsilon^{2-\alpha} \Psi(x)$ , where  $x = \delta n / \epsilon^\beta$  is a scaling variable combining the deviation from the critical density ( $\delta n$ ) and temperature ( $\epsilon$ ), while  $\Psi(x)$  is a universal scaling function and  $\alpha, \beta$  are critical exponents, respectively, known with high accuracy [23]. The precise definition of the scaling fields ( $\delta n, \epsilon$ ) in fluids is however rather subtle and involves field mixing: while in the nearest-neighbor lattice gas model  $\delta n$  and  $\epsilon$  have the usual meaning of reduced density and temperature, respectively, leading to a coexistence curve fully symmetrical with respect to the critical density, in a fluid the order parameter  $\delta n$  is generally a linear combination of reduced density and temperature. For these reasons in real fluids, and markedly in micellar suspensions, the binodal displays a strong asymmetry between the vapor and the liquid branch and the line  $x = 0$  is conveniently identified as the locus of maxima of the isothermal susceptibility  $\chi = \partial n / \partial \mu$ . A more detailed description of the theory can be found in [10]. In the critical region our theory leads to the scaling form for the effective force per unit surface of the two walls:

$$(9) \quad F(h) = \frac{k_B T}{h^3} \theta(x; h^{1/\nu} \epsilon).$$

The ratio  $Fh^3/k_B T$  is dimensionless, and in fact universal: the DFT approach, commonly adopted in colloid science, leads to the same scaling form predicted for the critical Casimir

effect showing that *depletion forces and critical Casimir effect have a common physical origin*. Our approach allows to express  $F(h)$  properties of a critical fluid also away from the critical isochore, where simulations have not been performed yet. Our results suggests that the Casimir force is small at  $x < 0$  and quickly grows as soon as  $x > 0$ . Therefore, we expect the line  $x = 0$ , which we have identified with locus of maxima of the isothermal susceptibility, to mark the transition between a region where Casimir forces are negligible ( $x < 0$ ) and a regime where they become relevant ( $x > 0$ ). This prediction is confirmed by our experimental data: fig. 2 shows that our transition line is close to the locus of the maxima of the isothermal susceptibility, experimentally measured by light scattering (scattering intensity is proportional to  $\xi$ ). Along this path, the quantity  $(\Pi - \Pi_c)\xi^3/k_B T$  of the surfactant solution is known to be constant, universal and equal to  $\sim 0.1$  [23], in remarkable agreement with the data in inset of fig. 2.

\* \* \*

We thank SOLVAY-SOLEXIS (Bollate, Italy) and ENI (S. Donato Milanese, Italy) for having kindly donated us the original particle and  $C_{12}E_8$  sample batches, C. BECHINGER, S. DIETRICH, D. FRENKEL, F. SCIORTINO and E. ZACCARELLI for useful discussions and comments, R. PIAZZA for helping us in the experimental work, J. COLOMBO and A. PAROLA for performing the hard theoretical work, and the Italian Ministry of Education and Research (MIUR) for PRIN 2008 funding.

## REFERENCES

- [1] DIJKSTRA M., BRADER J. M. and EVANS R., *J. Phys.: Condens. Matter*, **11** (1999) 10079.
- [2] ROTH R., EVANS R. and LOUIS L. L., *Phys. Rev. E*, **64** (2001) 051202.
- [3] CHARBONNEAU P. and REICHMAN D. R., *Phys. Rev. E*, **75** (2007) 011507.
- [4] BUZZACCARO S., RUSCONI R. and PIAZZA R., *Phys. Rev. Lett.*, **99** (2007) 098301.
- [5] NORO M. G. and FRENKEL D., *J. Chem. Phys.*, **113** (2000) 2941.
- [6] MILLER M. A. and FRENKEL D., *J. Chem. Phys.*, **121** (2004) 535.
- [7] ASAKURA S. and OOSAWA F., *J. Chem. Phys.*, **22** (1954) 1255.
- [8] BUZZACCARO S., PIAZZA R., COLOMBO J. and PAROLA A., *J. Chem. Phys.*, **132** (2010) 124902.
- [9] BUZZACCARO S., PIAZZA R., COLOMBO J. and PAROLA A., *Phys. Rev. Lett.*, **105** (2010) 198301.
- [10] PIAZZA R., BUZZACCARO S., PAROLA A. and COLOMBO J., *J. Phys.: Condens. Matter*, **23** (2011) 194114.
- [11] HERTLEIN S. C *et al.*, *Nature*, **451** (2008) 172.
- [12] CASIMIR H. B. G., *Proc. K. Ned. Akad. Wet.*, **51** (1948) 793.
- [13] FISHER M. E. and DE GENNES P. G., *C. R. Acad. Sci. Paris B*, **287** (1978) 207.
- [14] DEGIORGIO V. *et al.*, *Adv. Colloid Interface Sci.*, **48** (1994) 61.
- [15] CORTI M. and DEGIORGIO V., *J. Phys. Chem.*, **85** (1981) 711.
- [16] HUNTER R. J., *Foundation of Colloid Science*, 2nd edition (Oxford University Press, Oxford) 1991.
- [17] HOGG R., HEALY T. W. and FUERSTENAU D. W., *Trans. Faraday Soc.*, **62** (1966) 1638.
- [18] HANSEN J. and McDONALD I. R., *Theory of Simple Liquids*, 2nd edition (Elsevier, Amsterdam) 1986.
- [19] CORTI M., MINERO C. and DEGIORGIO V., *J. Phys. Chem.*, **88** (1984) 309.
- [20] ZULAUF M. *et al.*, *J. Phys. Chem.*, **89** (1985) 3411.
- [21] BORJAN Z. and UPTON P. J., *Phys. Rev. Lett.*, **101** (2008) 125702.
- [22] CURTIN W. A. and ASHCROFT N. W., *Phys. Rev. A*, **32** (1985) 2909.
- [23] PELISSETTO A. and VICARI E., *Phys. Rep.*, **368** (2002) 549.